www.elsevier.nl/locate/jorganchem
Journal of Organometallic Chemistry 592 (1999) 95–102

Reactions of metalloalkynes 5: reinvestigation of the reaction of $[\{Ru(CO)_2(\eta\text{-}C_5H_4R)\}_2(\mu\text{-}C{\equiv}C)]$ with $[Ru_3(CO)_{10}(\mu\text{-dppm})]$

Lindsay T. Byrne, James P. Hos, George A. Koutsantonis *, Brian W. Skelton,
Allan H. White

Department of Chemistry, University of Western Australia, Perth, Nedlands, WA, 6907, Australia

Received 12 July 1999; accepted 4 August 1999

Abstract

We have previously reported the reactions of the activated cluster compound, $[Ru_3(CO)_{10}(dppm)]$ (**1**), with ethyne-1,2-diyl compounds, $[\{Ru(CO)_2(\eta\text{-}C_5H_4R)\}_2(\mu\text{-}C{\equiv}C)]$, (**2a**, R = H; **2b**, R = CH_3), which gave the new complexes $[Ru_5(\mu_5\text{-}C{\equiv}C)(\eta\text{-}C_5H_4R)_2(dppm)(\mu_2\text{-}CO)_2(CO)_7]$, (**3a**, R = H; **3b**, R = CH_3). Our desire to extend the chemistry of these complexes required larger quantities of starting materials and in these syntheses we found that an additional complex, $[Ru_5(\mu_4\text{-}CC)(\eta\text{-}C_5H_5)_2(dppm)(\mu\text{-}CO)(CO)_9]$ (**4a**), was formed. This apparently results from the reaction of **1** with **2**, and is related to $[Ru_5(\mu_5\text{-}C{\equiv}C)(\eta\text{-}C_5H_5)_2(dppm)(\mu_2\text{-}CO)_2(CO)_7]$ (**3a**) by the addition of a single carbonyl ligand. The reaction of complex **3b** with CO was investigated and resulted in the isolation of $[Ru_4(\mu_4\text{-}C{\equiv}C)(\eta\text{-}C_5H_4Me)_2(dppm)(CO)_9]$ (**5b**) and the isolation of complex **4b**, which was identified by comparison of its spectroscopic properties with that of **4a**, in addition the ^{13}CO labelling of complexes **3** resulted in the unequivocal assignment of the carbide resonances in their ^{13}C-NMR spectra © 1999 Elsevier Science S.A. All rights reserved.

Keywords: Ruthenium; Cluster; Carbide; Tetranuclear; Pentanuclear

1. Introduction

We have been examining the chemistry of ethyne-1,2-diyl compounds in an effort to rationally build well-defined metal aggregates [1–5]. In an earlier paper [1] we reported that the reaction of $[Ru_3(dppm)(CO)_{10}]$ (**1**) with $[Ru(CO)_2(\eta\text{-}C_5H_4R)\}_2(\mu\text{-}C{\equiv}C)]$ (**2**) resulted in the formation of mainly one product, $[Ru_5(\mu_5\text{-}C{\equiv}C)(\eta\text{-}C_5H_4R)_2(dppm)(\mu_2\text{-}CO)_2(CO)_7]$, (**3a**, R = H; **3b**, R = CH_3) (Scheme 1). We were interested in the reactions of **3** with catalytically important reagents such as dihydrogen or carbon monoxide, expecting that these reactions would illuminate the possible transformations that bicarbide ligands undergo on metal surfaces.

Herein we report the characterisation of an intermediate complex that was identified en route to complexes **3**, and the reaction of these latter complexes with CO, and the further characterisation of complexes **3**.

2. Results and discussion

On a relatively small scale, the reaction of **1** with **2** consistently yielded 65–75% of the pentanuclear clusters, **3**. However, when performed on a larger scale, or under less forcing conditions, small quantities of a purple compound were obtained accompanying the major product; on a smaller scale these purple products were not isolatable. Column chromatographic separation of the products from a large-scale preparation and crystallisation of the eluted purple band enabled isolation of $[Ru_5(\mu_4\text{-}CC)(\eta\text{-}C_5H_5)_2(dppm)(\mu\text{-}CO)(CO)_9]$ (**4a**). Complex **4a** was fully characterised by a spectroscopic and X-ray crystallographic study (see below).

The solution IR spectrum of **4a** was similar to that of complex **3** and contained bands attributable to terminal and bridging CO ligands. The FAB MS of **4** contained a low-intensity molecular ion at *m*/*z* 1326. The base peak corresponded to $[M\text{–}RuC(CO)_2(C_5H_5)]^+$. The proton NMR spectrum showed two singlet resonances at 4.92 and 4.64 ppm, which were assigned to the

---

* Corresponding author. Fax: +61-9380-1005.
E-mail address: gak@chem.uwa.edu.au (G.A. Koutsantonis)

0022-328X/99/$ - see front matter © 1999 Elsevier Science S.A. All rights reserved.
PII: S0022-328X(99)00489-1

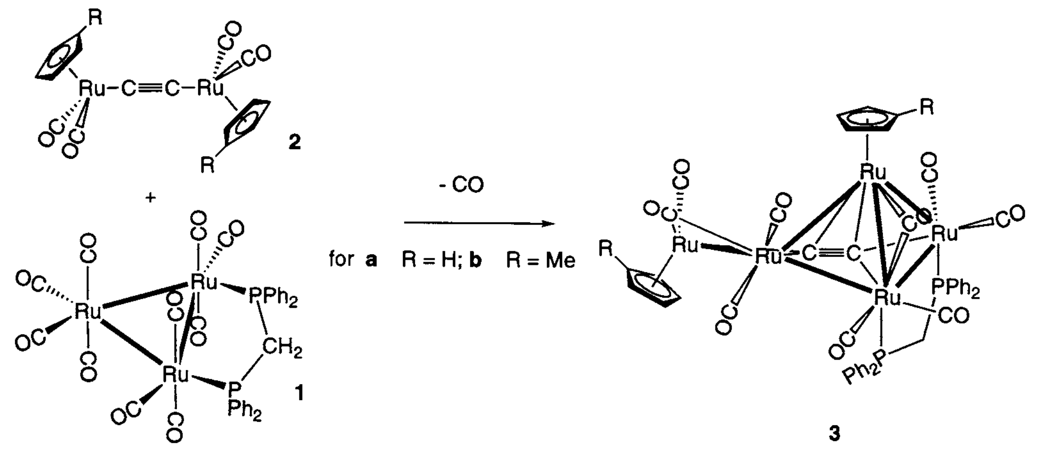

Scheme 1.

cyclopentadienyl ligands, accompanied by two analogously assigned peaks at 4.39 and 4.77 ppm of lesser intensity. The acquisition of a ^{13}C-NMR spectrum of complex **4** overnight was unsuccessful, with the sample becoming green in colour. Subsequently, the ^{1}H-NMR spectrum of the green solution revealed that the two sets of signals attributed to η^5-C_5H_5 resonances had swapped their intensities and the shifts of the now intense peaks were consistent with those of complex **3a**. Additionally, IR and thin-layer chromatographic analysis revealed that an almost quantitative transformation to **3a** had occurred.

The reaction of complexes **3** with dihydrogen proved to be unproductive with respect to the isolation of tractable compounds. However, carbon monoxide gas, bubbled slowly through a solution of **3b** in toluene, produced a colour change in a matter of minutes, the solution became eventually deep red–purple in colour. Conventional thin-layer chromatography proved unsuitable for purification as the products appeared to have limited stability under the conditions employed. Radial chromatography under argon allowed the separation of the mixture giving three bands, crystallised in moderate to low yields. The first minor yellow band eluted proved to be the dimeric $[Ru(CO)_2(\eta\text{-}C_5H_4Me)]_2$ (TLC, IR). The second yellow band was crystallised in low yield and structurally characterised (see below) as $[Ru_4(\mu_4\text{-}CC)(\eta\text{-}C_5H_4Me)(dppm)(CO)_9]$ (**5b**). Six terminal CO bands were observed in its solution IR spectrum. The ^{1}H-NMR spectrum contained resonances for η-C_5H_4Me and phenyl groups in the expected regions but the instability of **5b** in solution prevented further characterisation. The major purple product was eluted last; its spectroscopic data were comparable to that found for complex **4a** (NMR, IR), and it was found to convert readily to complex **3b** during attempted crystallisations, this hampering the collection of additional characterisational data.

It is of note that complexes **3** appear unreactive towards other two-electron donors and alkynes, such as PPh_3, PEt_3, Bu^tNC, PhC_2H and dimethylacetylenedicarboxylate. Given the relatively open geometry found in these complexes this result is surprising.

2.1. Solid-state structures of **4a** and **5b**

The results of the room-temperature X-ray structure determinations are presented (Figs. 1 and 2) with the relevant interatomic parameters in Table 1. Details of the structure solution and refinement are contained in Section 4 and Table 2.

In the course of the above work, occasion was had to check the identities of **3a** and **3b** by unit cell determinations. In each case a quite different cell was found, so that recourse was had to full structure determinations to ascertain the reason. In each case it transpired that the difference was due simply to a different mode of solvation from that originally recorded. Crystal data for these arrays is recorded below with full details being deposited, the results of the two determinations showing no non-trivial differences in respect of the core geometries of the two species.

Suitable specimens for X-ray diffraction were obtained from CH_2Cl_2–MeOH for **4a** (purple), and from CH_2Cl_2–pentanes for **5b**. The former crystallised in the monoclinic space group $P2_1/c$ and the latter in the orthorhombic space group *Pbcn*; one complete molecule and a disordered solvent molecule, and a complete molecule, unsolvated, respectively comprised the asymmetric units.

The attachment of the C_2 unit in both molecules **4a** and **5b** to the metal framework was in the ubiquitous μ_3:η^1:η^2-C≡CR bonding mode seen in a number of alkyne-derived metal clusters [6] of varying nuclearity. The coordination mode can be formally denoted in the following way, μ_4:η^1(Ru(2)):η^2(Ru(1)):η^2(Ru(3)):η^1-(Ru(n))–CC. The structure is comparable to that found

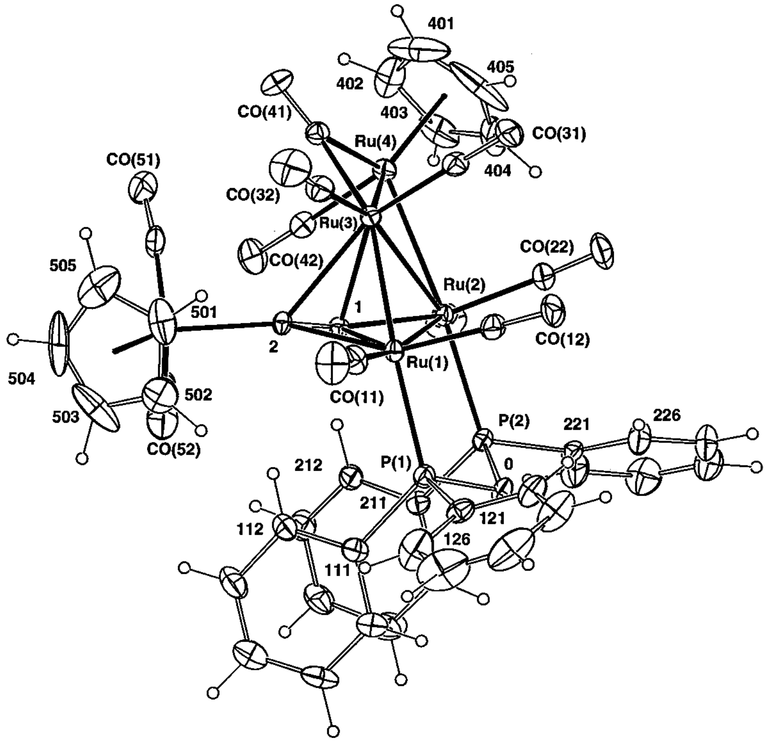

Fig. 1. Molecular structure of complex **4a**: 20% probability ellipsoids are shown for the non-hydrogen atoms here and for **5b**, hydrogen atoms having arbitrary radii of 0.1 Å.

in the bimetallic tetranuclear clusters [$Fe_2Ru_2(\mu_4$-$C{\equiv}C)(\mu$-$CO)(CO)_8(\eta$-$C_5H_5)_2$] [5] and [$Fe_2Co_2(\mu_4$-$C{\equiv}C)(CO)_6(\mu$-$CO)_2(\eta$-$C_5Me_5)_2$] [7], both derived from the reaction of ethyne-1,2-diyl complexes with metal substrates. The triangular metal motif to which the carbide ligand is bound varies between the structures of **4a** and **5b**; a slight elongation of ca. 0.09 Å in Ru(1)–Ru(2) and a contraction of ca. 0.2 Å in Ru(1)–Ru(3) is observed on going from **4a** to **5b**. Presumably this is the result of the steric effect of the additional metal atom in **4a** which has a bulky cyclopentadienyl ligand attached. The metal core geometry in **4a** has four ruthenium atoms adopting a flattened butterfly configuration and interacts with the C_2 ligand through one wing only. All five ruthenium atoms achieve 18-valence-electron counts. The C_2 ligand bridges the four metal atoms in an η^1(Ru(2)):η^2(Ru(4)):η^2(Ru(1)):η^1(Ru(5)) fashion, formally donating five electrons to the cluster framework. The metal–carbide bond distances in **4a** show slight variations when compared to **3a** and are similar to those of complex **5b**. The C≡C length C(1)–C(2) in **4b** is closer to that of **2** rather than that of **3a**, suggesting that some triple-bond character remains. This premise is supported by the Ru(5)–C(2) distance which is indicative of an Ru–C $\eta^1(\sigma)$-bond. In short, the mode of attachment of the C_2 unit, in both **4a** and **5b**, is analogous to that found in other acetylide clusters.

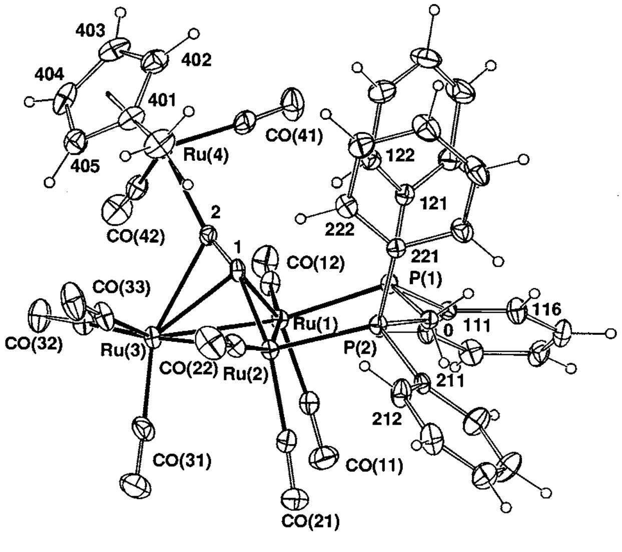

Fig. 2. Molecular structure of complex **5b**.

A formal electron count in **5b** shows that Ru(1), Ru(3) and Ru(4) achieve 18-electron counts and the remaining ruthenium atom has a 17-electron count.

2.2. Formation of the complexes

We have noted previously [1] that unlike many reactions of [$Ru_3(CO)_{10}$(dppm)] (**1**), the diphosphine ligand remains intact during the formation of the pentanuclear

Table 1
Selected bond distances (Å) and angles (°) for $[Ru_5(\mu_5\text{-}C{\equiv}C)(\eta\text{-}C_5H_5R)_2(dppm)(\mu_2\text{-}CO)_2(CO)_7]$ (**3a**), $[Ru_5(\mu_4\text{-}CC)(\eta\text{-}C_5H_5)_2(dppm)(\mu\text{-}CO)(CO)_9]$ (**4a**), and $[Ru_4(\mu_4\text{-}C{\equiv}C)(\eta\text{-}C_5H_4Me)_2(dppm)(CO)_9]$ (**5b**)

	3a [1]	**4a**	**5b**
Bond distances			
Ru(1)–Ru(2)	2.775(1)	2.8830(9)	2.7970(6)
Ru(1)–Ru(3)	2.738(1)	2.6191(8)	2.8158(6)
Ru(1)–Ru(4)	2.972(1)	–	–
Ru(2)–Ru(3)	2.838(1)	2.7421(8)	2.7647(6)
Ru(3)–Ru(4)	2.833(1)	2.7323(9)	–
Ru(4)–Ru(5)	2.777(1)	–	–
Ru(1)–C(1)	2.184(8)	2.245(6)	2.194(5)
Ru(1)–C(2)	2.702(8)	2.387(6)	2.382(5)
Ru(2)–C(1)	1.982(7)	1.994(7)	1.982(5)
Ru(3)–C(1)	2.165(6)	2.252(6)	2.217(4)
Ru(3)–C(2)	2.337(7)	2.459(7)	2.360(5)
Ru(4)–C(2)	2.134(7)	–	2.081(5)
Ru(5)–C(2)	2.066(8)	2.089(7)	–
Ru(1)–P(1)	2.321(2)	2.296(2)	2.326(1)
Ru(2)–P(2)	2.286(2)	2.335(2)	2.288(1)
C(1)–C(2)	1.29(1)	1.26(1)	1.292(7)
Bond angles			
Ru(1)–Ru(2)–Ru(3)	58.38(3)	55.43(2)	60.83(2)
Ru(1)–Ru(3)–Ru(2)	59.66(3)	65.01(2)	60.15(1)
Ru(2)–Ru(1)–Ru(3)	61.97(2)	59.56(2)	59.02(2)
Ru(1)–Ru(4)–Ru(5)	106.26(3)	–	–
Ru(3)–Ru(4)–Ru(5)	90.96(3)	–	–
Ru(2)–C(1)–Ru(3)	86.2(3)	80.2(2)	82.2(2)
Ru(2)–C(1)–Ru(1)	83.4(2)	85.5(2)	83.9(2)
Ru(4)–C(2)–Ru(5)	82.7(3)	–	–
Ru(2)–C(1)–C(2)	166.1(5)	161.4(5)	158.8(4)
Ru(4)–C(2)–C(1)	125.1(6)	–	–
Ru(5)–C(2)–C(1)	152.0(6)	–	–
Ru(3)–C(2)–Ru(4)	78.5(2)	–	126.6(2)
Ru(3)–C(2)–Ru(5)	130.5(3)	–	–

complexes **3**, perhaps a consequence of the templating ability of the C_2^{2-} ligand in these systems. The isolation of **4a** is significant and allows us to speculate further on the course of the reaction between the ethyne-1,2-diyl complexes **1** and cluster **2** (Scheme 2). This enhanced reactivity of **1** over $[Ru_3(CO)_{12}]$ results from steric strain induced at the un-substituted Ru atom in **1** by the presence of the dppm ligand bridging a Ru–Ru bond. This has the ultimate effect of labilising an equatorial carbonyl on the un-substituted Ru atom, allowing ready substitution at this position. Two possible mechanisms have been proposed for substitution of **1**. In the one nucleophilic substitution can occur at a vacant coordination site; in the other rapid associative substitution occurs at the generated 17-electron $Ru(CO)_4$ moiety [8,9].

The connectivity of **4a** suggests that the addition of **2a** to the triangular Ru_3 core of **1** occurs without significant disruption of the framework. Subsequently, the migration of a $[Ru(CO)_2(\eta\text{-}C_5H_5)]$ moiety occurs with concomitant formation of two metal–metal bonds and the coordination of the C_2 unit to the metal frame in a bridging fashion. The final process is one of carbonyl loss from **4a** to generate **3a**. It is possible that the proximity of protons on the cyclopentadienyl ligand and on one of the phosphine phenyl rings in **4a** (contact distance, PPh–H(112)···C–H(502), ca. 2.688 Å) provide the impetus for further condensation and expulsion of CO giving ultimately complex **3a**.

The mechanism of formation of **5b** is somewhat problematic. The observation of complex **4b** in the reaction of **3b** with carbon monoxide, from which **5b** is isolated, is unusual given our previously mentioned results with other two-electron donors but implies that the addition of CO to both complexes **3** is reversible (Scheme 3). Thus, further reaction of **4b** with CO must induce cluster break-up and this premise is supported by the isolation of $[Ru(CO)_2(\eta\text{-}C_5H_5)]_2$ from the reaction mixture.

2.3. *NMR investigation of isotopically enriched* $[Ru_5(\mu_5\text{-}CC)(\eta\text{-}C_5H_5)_2(dppm)(\mu\text{-}CO)_2(CO)_7]$ *(**3a**)*

The assignment of the NMR signals arising from the presence of carbonyl and carbide ligands is often difficult [6,10] as in general they are of a low intensity. One strategy for assignment is the isotopic enrichment of the complexes using either ^{13}C-carbon monoxide or ^{13}C enrichment of the C(sp) of the ethyn-1,2-diyl ligand. We prepared $[\{^{13}CO\}\text{–}Ru_3(CO)_{12}]$ by exchange in toluene under an atmosphere of $^{13}CO_{(g)}$ and subsequently $[^{13}CO]$-**1**. It was not feasible to attempt an exchange on **1** directly as the increased temperatures would result in unwanted side reactions [11]. This then allowed us to prepare the appropriately enriched $[^{13}CO]$-**3a**.

The analysis of cyclopentadienyl:carbonyl peak ratios between enriched and un-enriched samples implied that the enrichment was in excess of 20%. We were thus able to unambiguously assign the resonances observed at 184.6 and 183.9 ppm to the carbide ligand. They were much smaller in intensity and had obviously not undergone ^{13}CO exchange.

The complex $[^{13}CO]$-**3a** was found to be stereochemically rigid on the NMR timescale down to 213 K and had a spectrum consistent with its solid-state structure containing resonances for all nine unequivalent carbonyl ligands. Five of the carbonyl resonances show coupling to the ^{31}P nuclei, coupling constants ranging from 6.5 to 38 Hz. The $^{31}P\{^1H\}$-NMR spectrum of $[^{13}CO]$-**3a** contains two resonances: one a broadened doublet at 36.8 ppm ($^1J_{CP} = 40$ Hz) which is similar to that found for the unenriched sample and the second resonance, is a complex 12-line multiplet centred at 31.5 ppm. The geometry around Ru(2) suggests that there should be no significant coupling of P(2) with the adjacent ^{13}C carbonyl ligands (Karplus relation [12]) and thus can be assigned to the signal arising from P(2). The carbonyl ligands on Ru(4) and Ru(5) are unlikely to couple to the remote phosphorus nuclei and are assigned to the singlets observed at 201.2, 208.5, 211.8 and 248.6 ppm in $^{13}C\{^1H\}$-NMR spectrum. The remaining carbonyls, viz. CO(11), CO(12), CO(31), CO(41) and CO(42) (Fig. 3), show phosphorus coupling, presumably to P(1), and signals were observed at 200.2, 207.3, 209.5, 211.5 and 212.7 ppm. The angle P(1)–Ru(1)–CO(31) of 168.3(2)° taken from the solid state structure suggests, on the basis of the Karplus relation, that the magnitude of the constant expected

Table 2
Crystal data/refinement details

Compound	**3a**	**3b**	**4a**	**5b**
Formula	$C_{46}H_{32}O_9P_2Ru_5$	$C_{48}H_{36}O_9P_2Ru_5 \cdot CH_2Cl_2$	$C_{47}H_{30}O_{10}P_2Ru_5 \cdot CH_2Cl_2$	$C_{42}H_{29}O_9P_2Ru_4$
Molecular weight	1296.1	1409.0	1407.0	1143.9
Crystal system	Triclinic	Orthorhombic	Monoclinic	Orthorhombic
Space group	$P\bar{1}$ (no. 2)	*Pbca* (no. 61)	$P2_1/c$ (no. 14)	*Pbcn* (no. 60)
a (Å)	11.195(2)	17.623(1)	12.4408(2)	21.663(2)
b (Å)	13.509(2)	22.338(1)	12.9025(6)	20.449(1)
c (Å)	15.295(3)	27.400(2)	32.728(2)	18.531(1)
α (°)	72.568(3)			
β (°)	80.507(3)		95.752(2)	
γ (°)	77.474(3)			
V (Å^3)	2142	10785	5227	8229
Z	2	8	4	8
Specimen (mm)	0.23 × 0.22 × 0.17	0.55 × 0.20 × 0.05	0.22 × 0.22 × 0.08	0.20 × 0.12 × 0.04
N_t	25329	114814	26912	91970
N_u (R_{int})	10161 (0.045)	13998 (0.029)	13790 (0.030)	10644 (0.037)
N_o	7052	8854	7961	5540
R	0.052	0.040	0.055	0.040
R_w	0.058	0.042	0.059	0.018
n_v	559	632	617	514
T (K)	153	300	300	300

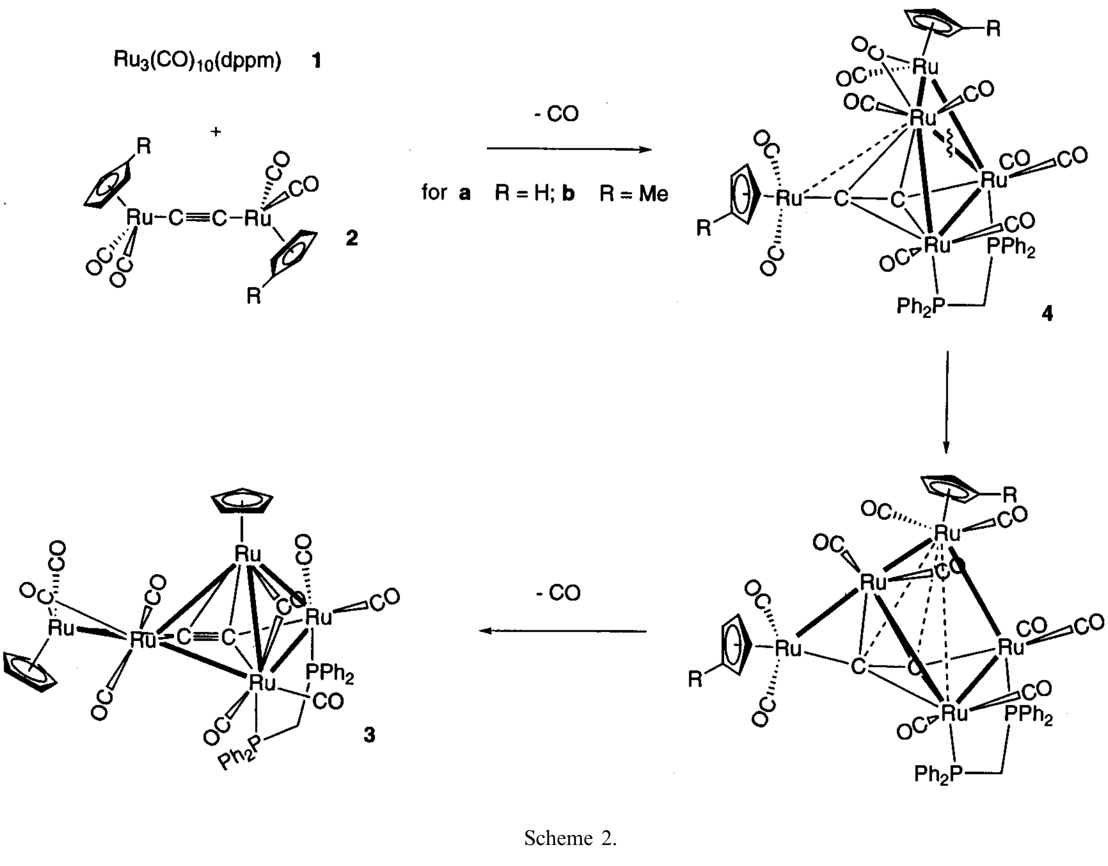

Scheme 2.

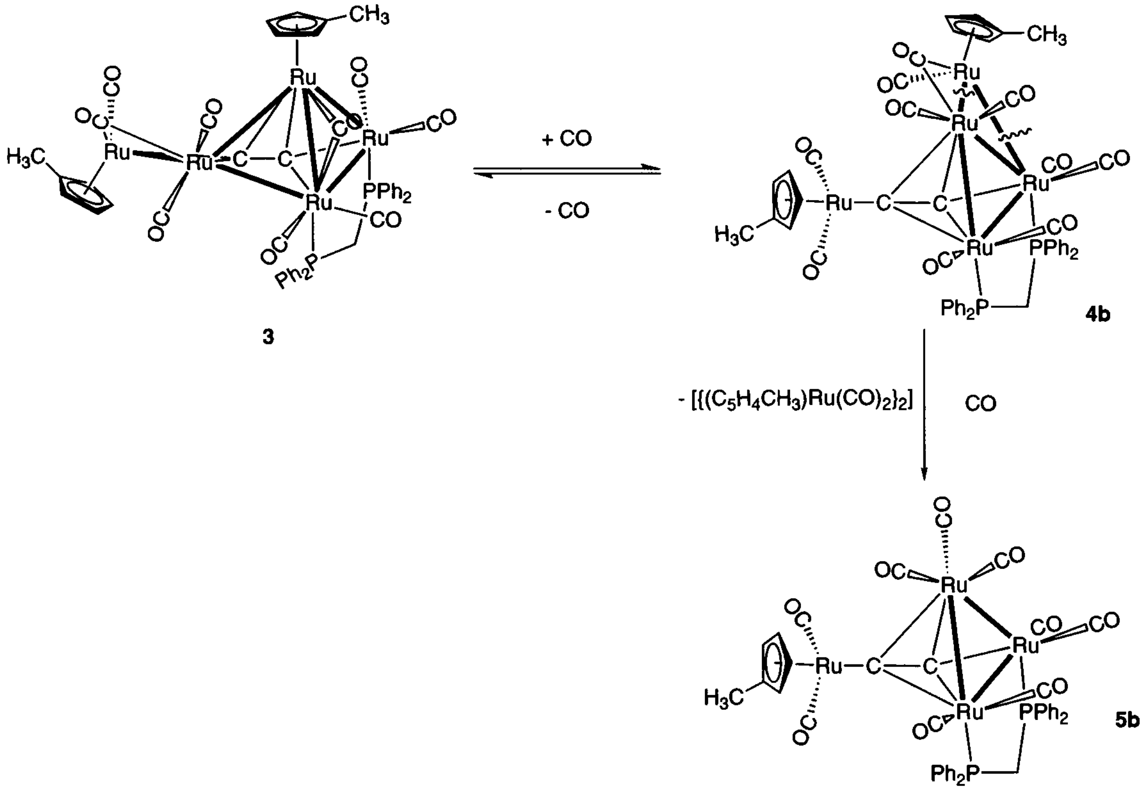

Scheme 3.

for this coupling should be the greatest of the couplings observed so that the signal observed at 209.5 ($J_{CP} = 38$ Hz) in the $^{13}C\{^1H\}$-NMR spectrum can be assigned to CO(31).

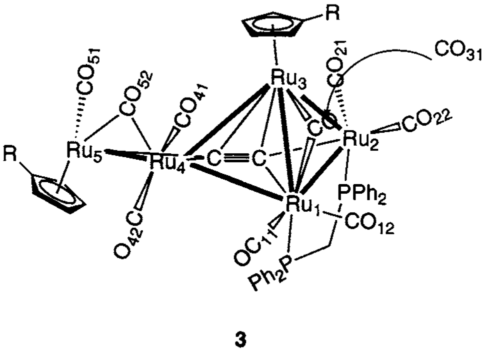

3

Fig. 3. Diagram showing atom labelling scheme used in complexes **3**.

3. Conclusions

The reactions of $[Ru_3(CO)_{10}(dppm)]$ with ruthenium ethyne-1,2-diyl compounds proceed through relatively complex mechanisms that have been somewhat illuminated by the observation of an intermediate complex containing an extra carbonyl ligand enroute to complexes $[Ru_5(\mu_5\text{-}C{\equiv}C)(\eta\text{-}C_5H_4R)_2(dppm)(\mu_2\text{-}CO)_2(CO)_7]$. Loss of this ligand provides the previously observed complex and the loss of the CO ligand appears to be reversible.

The unequivocal assignment of ^{13}C-NMR resonances associated with carbide ligands can only be achieved by the use of labelling experiments.

4. Experimental

4.1. General conditions

The manipulation of oxygen- and moisture-sensitive compounds was performed under an atmosphere of high-purity argon using standard Schlenk techniques or in a dry box (Miller–Howe).

Infrared spectra were recorded using a Bio-Rad FTS 45 FTIR spectrometer. Spectra were acquired either in solution (CsI cell), as nujol mull (NaCl discs) or pellet (KBr).

^1H- and ^{13}C-NMR spectra were acquired using Varian Gemini 200 (^1H at 200 MHz and ^{13}C at 50.3 MHz), or Bruker ARX 500 (^1H at 500.13 MHz and ^{13}C at 125.8 MHz) spectrometers. ^{31}P-NMR spectra were acquired using a Bruker ARX 500 (202.5 MHz) instrument. NMR spectra were referenced with respect to solvent signals.

Mass spectra were obtained on a VG AutoSpec spectrometer employing a fast atom bombardment (FAB) ionisation source (Cs^+, 20 keV) in all samples unless otherwise specified. FAB mass spectra are reported in the following form: m/z ([assignment]$^+$, % of base peak)

The Research School of Chemistry Microanalytical Unit, Australian National University, performed elemental analyses.

Tetrahydrofuran (BDH), and diethyl ether (Ajax) were dried over Na–K alloy and distilled from potassium benzophenone ketyl under an atmosphere of argon. Toluene (Ajax) was dried over sodium metal and distilled from sodium benzophenone ketyl under an atmosphere of argon. Pentanes (BDH) and hexane (Ajax) were dried over sodium metal and distilled under an atmosphere of argon. Silica (BDH) and aluminium oxide (Fluka 5016 A Basic and Neutral) were used for column chromatography. A 1 mm or 0.5 mm thickness of Silica Gel GF_{254} (Fluka) was used to coat preparative TLC Plates (20 × 20 cm). 0.5 mm of Silica Gel PF_{254} was used to coat radial chromatography plates.

4.2. Starting materials

The complexes $[Ru_3(CO)_{12}]$ [13], $[Ru_3(CO)_{10}(dppm)]$ [14], $[\{Ru(CO)_2(\eta\text{-}C_5H_5)\}_2(\mu\text{-}C{\equiv}C)]$ [4] were prepared by literature methods.

*4.3. Reaction of $[\{Ru(CO)_2(\eta\text{-}C_5H_5)\}_2(\mu\text{-}C{\equiv}C)]$ (**2a**) with $[Ru_3(dppm)(CO)_{10}]$ (**1**); preparation of $[Ru_5(\mu_4\text{-}CC)(\eta\text{-}C_5H_5)_2(dppm)(\mu\text{-}CO)(CO)_9]$ (**4**)*

A solution of (**1a**), (250 mg, 0.534 mmol) and (**2**), (500 mg, 0.517 mmol) in THF was refluxed (14 h). Solvent was removed in vacuo and the residue applied to alumina (neutral Act. IV), (30 × 3 cm). Elution with 10% CH_2Cl_2–n-hexane yielded a red–orange band, $Ru_3(CO)_{10}(dppm)$ (72 mg, 0.074 mmol) identified by comparison with an authentic sample. Elution with 30% CH_2Cl_2–n-hexane yielded a purple band which, after recrystallisation (CH_2Cl_2–MeOH) gave small dark purple crystals of (**4**)·$0.5CH_2Cl_2$, (14 mg, 4.2%). Anal. Calc. for $C_{52}H_{42}Cl_{10}O_{10}P_2Ru_5$: C, 35.71; H, 2.42. Found: C, 35.92; H, 2.57%; IR (CH_2Cl_2) ν(CO) 2050 m, 2001 vs, 1998 s, 1949 vs, 1899 w, 1783 m cm^{-1}; ^{1}H-NMR $\delta(C_6D_6)$ 2.4 (m, 1H, $P_xCH_aH_bP_y$), 3.75 (m, 1H, $P_xCH_aH_bP_y$), 4.64 (s, 5H, C_5H_5), 4.92 (s, 5H, C_5H_5), 6.6–7.8 (m, 20H, $2\times Ph_2PCH_2$); FAB MS (NOBA/CH_2Cl_2) m/z 1326 ([M]$^+$, 3.5%), 1102 ([M–CpRu$(CO)_2$C]$^+$, 100%), 1074 ([M–CpRu$(CO)_2$C–CO]$^+$, 10%). Elution with 45% CH_2Cl_2–n-hexane yielded a green band, of the previously characterised complex (**3a**) (255 mg, 74%).

*4.4. Reaction of $[Ru_5(\mu_5\text{-}CC)(\eta\text{-}C_5H_4Me)_2(dppm)(\mu\text{-}CO)_2(CO)_7]$ (**3b**) with $CO_{(g)}$, characterisation of $[Ru_4(\mu_4\text{-}CC)(\eta\text{-}C_5H_4Me)(dppm)(CO)_9]$ (**5**)*

A dark green solution of (**3b**) (45 mg, 36 μmol) in toluene was stirred under a gentle purge of $CO_{(g)}$ (~ 1 bubble s^{-1}). After several hours the colour changed to deep red. Similar results were obtained by performing the reaction under ca. 10 atm $CO_{(g)}$ in a high-pressure autoclave. After 14 h the solvent was removed in vacuo and the residues separated by radial chromatography using acetone–n-hexane. A yellow band was first collected and crystallised (CH_2Cl_2–n-hexane) to give light yellow crystals of $[Ru(\eta\text{-}C_5H_4Me)(CO)_2]_2$ (2 mg, 4.7%) (IR). A second yellow band was collected (ca. 15% acetone–hexane) and crystallised (CH_2Cl_2–pentanes) to give yellow crystals of (**5**), (2 mg, 9%). IR (CH_2Cl_2) ν(CO) 2048 m, 1996 s, 1955 m, 1931 sh w, 1767 m cm^{-1}; ^{1}H-NMR $\delta(CD_2Cl_2)$ 4.18 (m, 2H, $P_xCH_aH_bP_y$), 5.29 (s, 5H, C_5H_5), 7.2–7.8 (m, 20H, $2\times P(C_6H_5)_2$). The major purple band was eluted (ca. 30% acetone) and recrystallised (CH_2Cl_2–n-hexane) to give purple crystals of (**4b**), (15 mg, 54%). A number of smaller bands were observed but not collected.

4.5. ^{13}CO enrichment of $[Ru_3(CO)_{12}]$

A suspension of $Ru_3(CO)_{12}$ (208 mg, 0.296 mmol) in toluene was frozen (77 K) in a 100 ml Schlenk flask fitted with a RotaFlow tap. The vessel was evacuated (diffusion pump) and ca. 1 atm of 99% $^{13}CO_{(g)}$ (Cambridge) was admitted. The sealed vessel was allowed to come to room temperature and was then stirred cautiously for 3 days at ca. 65°C. Exchange was confirmed by IR.

5. Structure determinations

Full spheres of area-detector diffraction data were measured at ca. 300 K using a Bruker AXS CCD instrument fitted with monochromatic Mo–K_α radiation source ($\lambda = 0.7107_3$ Å) within the limit $2\theta_{max} = 58°$. $N_{t(otal)}$ reflections were acquired, reducing to N unique (R_{int} quoted) using the proprietary software SMART/SAINT/SADABS/XPREP incorporating empirical absorption corrections, N_o of these with $F > 4\sigma(F)$ being used in the full matrix least squares refinements. Anisotropic thermal parameters were refined for the non-hydrogen atoms, $(x, y, z, U_{iso})_H$ being included constrained at estimated values. Conventional residuals on $|F|$, R, R_w (statistical weights) are quoted at convergence. Neutral atom complex scattering factors were employed, computation using the Xtal 3.4 program system [15]. Pertinent results are given in the

Figures and Tables, atomic coordinates being deposited with the Cambridge Crystallographic Data Base (deposition numbers CCDC 130238–CCDC 130241). For both **3b** and **4a**, difference map residues, presumed solvent, were modelled in terms of a pair of molecules with constrained geometries, site occupancies set at 0.5 after trial refinement.

Acknowledgements

We thank the Australian Research Council and the Special Research Centre for Materials and Minerals Processing, UWA, for supporting this work. J.P.H. is the holder of an Materials Institute of Western Australia Scholarship. We thank Dr Allan McKinley and his group for use of a high-vacuum line.

References

[1] L.T. Byrne, C.S. Griffith, J.P. Hos, G.A. Koutsantonis, B.W. Skelton, A.H. White, J. Organomet. Chem. 565 (1998) 259.
[2] L.T. Byrne, C.S. Griffith, G.A. Koutsantonis, B.W. Skelton, A.H. White, J. Chem. Soc. Dalton Trans. (1998) 1575.
[3] C.S. Griffith, G.A. Koutsantonis, B.W. Skelton, A.H. White, Chem. Commun. (Cambridge) (1998) 1805.
[4] G.A. Koutsantonis, J.P. Selegue, J. Am. Chem. Soc. 113 (1991) 2316.
[5] G.A. Koutsantonis, J.P. Selegue, J.-G. Wang, Organometallics 11 (1992) 2704.
[6] P.R. Raithby, M.J. Rosales, Adv. Inorg. Chem. Radiochem. 29 (1986) 169.
[7] M. Akita, Y. Morooka, Bull. Chem. Soc. Jpn. 68 (1995) 420.
[8] B. Ambwani, S.K. Chawla, A.J. Poe, Inorg. Chim. Acta 133 (1987) 93.
[9] B. Ambwani, S.K. Chawla, A.J. Poe, Polyhedron 7 (1988) 1939.
[10] M.I. Bruce, Coord. Chem. Rev. 166 (1997) 91.
[11] M.I. Bruce, P.A. Humphrey, B.W. Skelton, A.H. White, M.L. Williams, Aust. J. Chem. 38 (1985) 1301.
[12] J.L. Marshall, Carbon–Carbon and Carbon Proton Couplings, vol. 2, Verlag Chemie, Deerfield Beach, FL, 1983.
[13] M.I. Bruce, C.M. Jensen, N.L. Jones, Inorg. Synth. 26 (1990) 276.
[14] M.I. Bruce, B.K. Nicholson, M.L. Williams, Inorg. Synth. 26 (1990) 225.
[15] S.R. Hall, G.S.D. King, J.M. Stewart, The XTAL 3.4 User's Manual, University of Western Australia, Lamb, Perth, 1995.